TABLE OF CONTENTS

LIST OF FIGURES

I. INTRODUCTION

The SLICE vessel concept was born out of the small waterplane area twin hull (SWATH) hull configuration which have better stability characteristics than a conventional mono hull of similar displacement [1]. The SWATH hull design consists of two submerged pods which provide the buoyancy of the vessel and may contain various pieces of propulsion or auxiliary machinery, fuel and water tanks or storage spaces. The pods may be cylindrical bodies of revolution, similar to a bare submarine hull, or may be some other shape. In either case the major portion of the vessel static stability comes from the submerged pods. The pods are connected to the working area of the ship by means of either single or multiple struts. At this point in time there are no standard SWATH configurations. Because all of the buoyancy comes from the pods and not the connecting struts they must have a large lateral separation to achieve static stability. This large separation results in a ship with a much wider beam and shorter length than that of a conventional mono-hull of equal displacement. As already mentioned the struts provide very little additional buoyancy which result in the pods being deeply submerged giving a much deeper draft than that of a conventional mono-hull of similar displacement. [1]

The primary benefit of the SWATH hull form is the excellent seakeeping ability resulting from the deep draft and wide beam. The SWATH hull form has pitch, roll and heave characteristics of vessels of much larger displacements providing for a better man-vessel interface in heavier seas. The man-vessel interface is defined as the ability of crew

members to perform all the vessel functions without suffering from the effects of sea-sickness or being swept overboard by a rogue wave, and trying to maintain one's balance while working in heavy seas. The wide beam may leave larger open deck space giving the planner or designer more flexibility in placement of deck fittings or machinery. The vessel's shorter length may give the captain a better overall view of the working deck area allowing swifter and more efficient command of operations on deck. While the shorter length may be considered as an advantage it comes at a cost of tendency to pitching due to a relatively small longitudinal metacentric height (GM_L).[1]

A. MANEUVERING AND CONTROL

In addition to its superior seakeeping ability, the SWATH hull is also directionally very stable, a direct result of the deep drafts and large underwater hull profile area. Conventional mono-hulls may require the addition of a rudder, fin or deadwood in order to achieve directional stability whereas the SWATH concept hulls, which are in essence large fins or wings, are exceptionally stable directionally at low speeds and increasingly so as flow over the hull increases. This increased stability also has its drawback because along with the ability to keep a straight course in seas or wind, it requires a much larger yawing moment to turn. At lower speeds this large yaw moment can be overcome with maneuvering thrusters or by differential thrust between the engines. At higher speeds the differential thrust is not as effective and the rudders must provide the necessary moment to initiate the turn. [1]

Rudders in use in current SWATH concept ships are standard balanced, horn or spade rudders and are placed aft as in a conventional mono-hull design. They are attached to the strut or haunch above and behind the screw as shown in Figure 1. The rudder's effectiveness is increased by placing it in the propeller wash. [1]

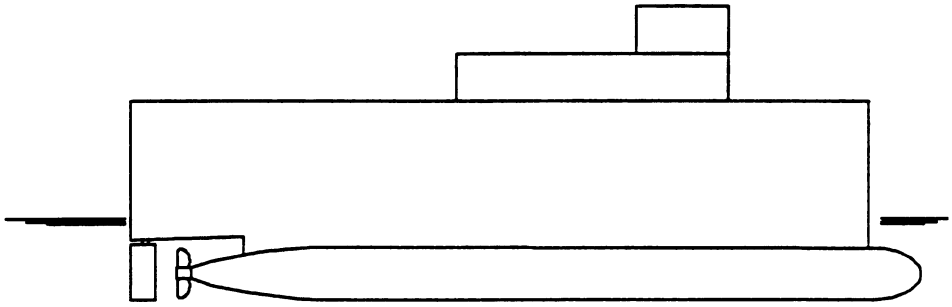

Figure 1. Conventional SWATH hull. [1]

B. THE SLICE HULL FORM

The SLICE hull differs from the SWATH hull in that the SLICE consists of two pods on each side providing buoyancy and stability versus one as in the SWATH hulls. Figure 2 shows a profile view of the SLICE with major dimensions and without rudders. Figure 3 is a stern view , diagram of the SLICE vessel without rudders or stabilizing fins, showing fore and aft pod offsets. In terms of maneuvering ability the SLICE presents some challenges in the location of the rudders. Should the rudders be placed in the propeller wash increasing the effectiveness of the rudder but reducing the turning moments created by such a rudder? Should they be placed on the after pod? The after

strut? Perhaps on the leading edge of the aft strut to place it somewhat in the propeller wash but increasing the moment it can create or even on the leading edge of the fore strut.

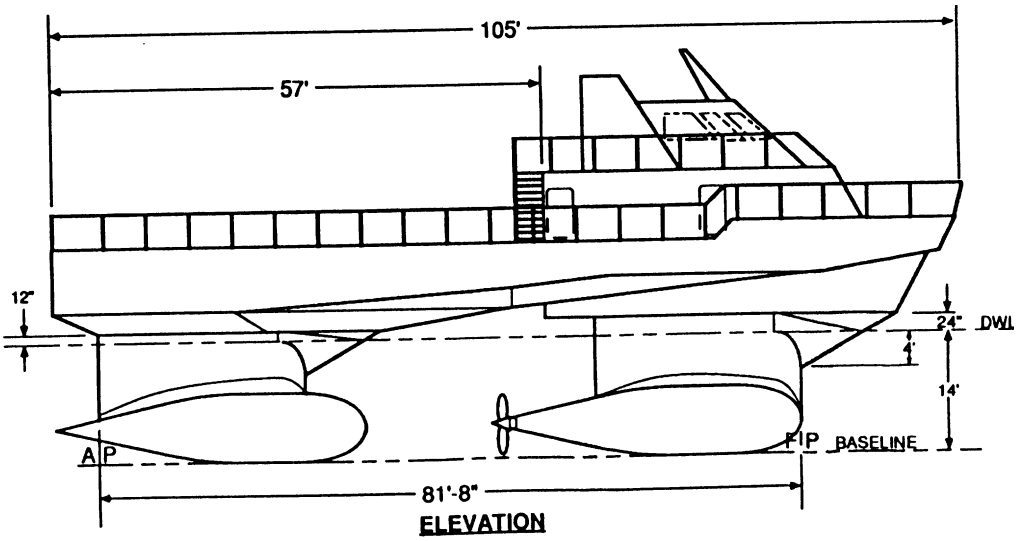

Figure 2. Profile view of SLICE vessel. [2]

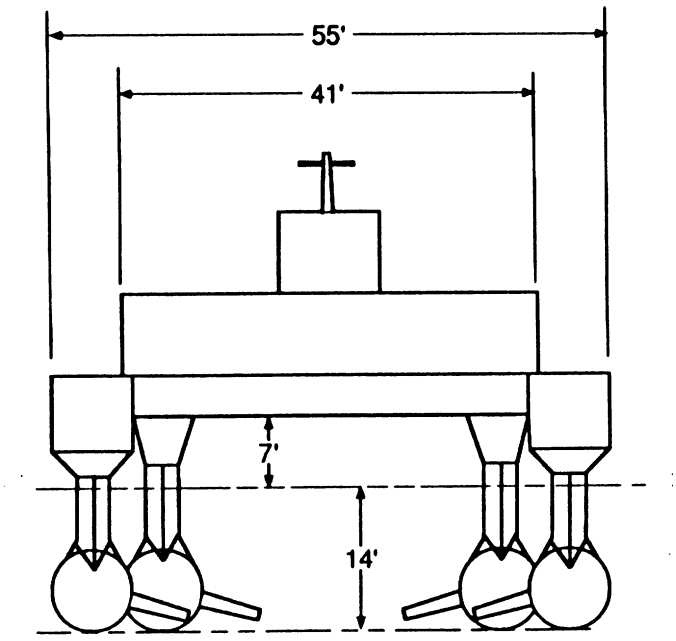

Figure 3. Stern view of SLICE [2].

II. DETERMINATION OF HYDRODYNAMIC COEFFICIENTS OF SLICE PODS

A. EQUATIONS OF MOTION FOR A SUBMERGED BODY IN THE HORIZONTAL PLANE: STEERING SYSTEM EQUATIONS

The equations of motion for a submerged body in the horizontal plane are similar in nature to that of an airplane in flight. The vehicle is assumed to be in steady state motion in calm seas without the effects of currents and waves. All steering system dynamics terms are referenced to a body fixed, orthogonal coordinate system with the origin fixed at the ship's reference point, which is usually fixed at the amidships main deck but can be chosen to be at any point. The x axis is fixed to the longitudinal center of the ship and is positive forward. The y or lateral axis is positive to starboard and the z axis is positive in the downward direction relative to the ship. [3,4,5]

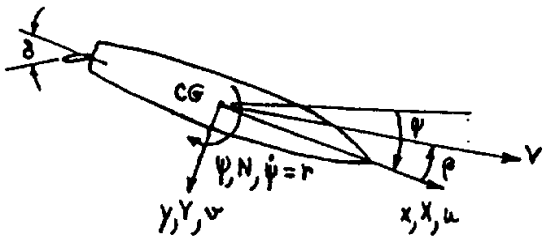

Figure 4. Body fixed axes [5]

For a vehicle with a high aspect ratio such as a surface ship, the forces are predominantly forces of lift developed as a result of the relative motion of the vessel and

the fluid. The longitudinal forces of drag, while important for the determination of power requirements are neglected for steering system dynamics. It is assumed that no loss of speed takes place in maneuvering. In straight line motion the lift forces on each side of a body which is symmetric about a longitudinal axis are equal and sum to zero. When the fluid impinging on the vessel has an angle of attack with respect to the longitudinal axis, then the lift forces are no longer in balance and dynamic forces are developed. In other words when the vessel has a side slip velocity component (v) in the y-direction an angle of attack relative to the fin or strut is caused. The angle of attack (α) is defined as v/U for small v and it gives rise to the lift forces and moments on the vessel hull. The ability of the hull to maintain a straight line path, in other words straight line stability, will be measure a of the stability of that particular hull form. The linearized sway and yaw equations of motion for a vessel in the horizontal plane are fully developed in Principles of Naval Architecture [3,4] and repeated here in matrix form as: [3]

$$\begin{bmatrix} m' - Y'_{\dot{v}} & -Y'_{\dot{r}} \\ -N'_{\dot{v}} & I'_{zz} - N'_{\dot{r}} \end{bmatrix} \begin{bmatrix} \dot{v} \\ \dot{r} \end{bmatrix} = \begin{bmatrix} Y'_{v} & Y'_{r} - m' \\ N'_{v} & N'_{r} \end{bmatrix} \begin{bmatrix} v \\ r \end{bmatrix} \tag{1}$$

Equation 1 is often more conveniently represented in matrix form as:

$$M\dot{x} = Ax \tag{2}$$

The components of the M and A matrices of equation 2 represent the linearized hydrodynamic derivatives of the forces developed by sideslip (v) and yawing (r) motions of the ship. Coefficients m' and I_{zz}' are the non-dimensionalized mass and mass moment of inertia of the vessel about the z axis. The forces developed, in their linearized form are represented as the derivative times the motion. In other words Y_v'v represents the lateral force developed by the side slip velocity v and Y_r'r represents the lateral force developed by the yawing motion r. In similar fashion the moments N_v'v and N_r'r represent the moments on the vessel about the selected reference point resulting from the lateral velocity and yawing motion. [3]

In order to fully study the steering system dynamics the effects of the rudder must be added to equation 2 as follows.

$$M\dot{x} = Ax + B\delta \tag{3}$$

Where B is a vector containing the linearized lateral force and moment contributions of the rudders as shown in equation 3 and δ is the angular displacement of the rudder (- for right rudder, + for left rudder for standard stern rudder).

$$B = \begin{bmatrix} Y'_{\delta} & N'_{\delta} \end{bmatrix} \tag{4}$$

In determining the controls fixed stability of a hull shape it is the eigenvalues of equation 2, re-written as

$$\dot{x} = \left[M^{-1} A \right] x \tag{5}$$

that represent a measure of the controls fixed stability of the ship. Controls fixed stability is the stability associated with a straight line path of the vessel with zero rudder angles. Complex conjugate eigenvalues with negative real parts correspond to a directionally stable vessel but with oscillatory response characteristics as shown in Figure 5 case IIA. Real, negative eigenvalues will be directionally stable with no oscillations as in case IIB. One or more positive eigenvalues indicate a hull form that is directionally unstable. [3,4]

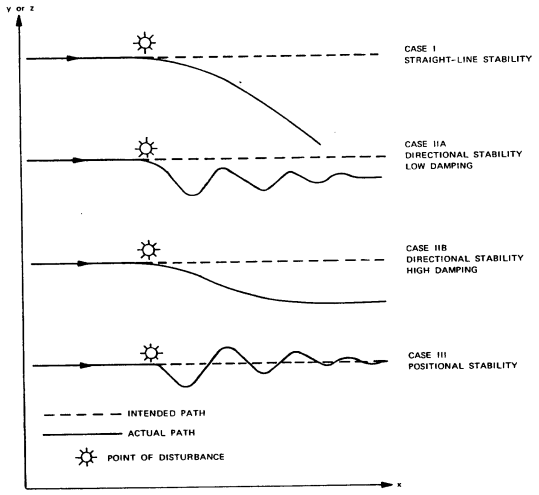

Figure 5. Motion stability of surface ships. [4]

B. ESTIMATION OF HYDRODYNAMIC COEFFICIENTS FOR A BODY OF REVOLUTION USING SEMI-EMPIRICAL METHODS

There are several different methods for estimation of the hydrodynamic coefficients for a submerged bodies of revolution relying on some semi-empirical relation to account for viscous or vortex effects on the body. The methods considered for the SLICE pods are summarized in a concise and comprehensive report from the Naval Coastal System Center [6]. It includes methods from United States Air Force Data Compendium, (USAF DATCOM), Naval Coastal Systems Center (NCSC) and Naval Ship Research and Development Center (NSRDC). While each agency has published several reports on the subject, Peterson [6] outlines the strengths and weaknesses of each of the above mentioned methods. Comparison of the various methods is made for both submarine shaped and torpedo shaped bodies of revolution developed by each source [6]. The acceleration hydrodynamic coefficients will be calculated by the methods of Humphreys and Watkinson [7].

All of the methods discussed are easily calculated both by hand and are amenable to computerized calculations [6]. However the methods of DATCOM and NCSC rely primarily on geometric considerations. Methods that required body masses or mass distributions such as NSRDC methods are discounted at this preliminary point in the modeling process as they are not as well defined or determined as the physical dimensions of the SLICE pods. [6]

Because of a lack of captive model tests or full scale maneuvering trial data it is necessary to build the computer model of the SLICE hull form in several parts. The first part is the pod itself which resembles a submarine form and is fully described below. Attached to each of the pods is the strut connecting the pod to the box. Struts are modeled as a flat plate fixed fin attached to the pod. The hydrodynamic coefficients of each strut/pod combination will be calculated individually for each pod with the reference point for moment coefficients taken at the pod mid length point. The effects of each of the four strut/pod configurations will then be non-dimensionalized with respect to the vessel length between perpendiculars (L_{bp}) and translated to the ships reference point and combined to get the total coefficients for the ship. [3]

While the SLICE pod form is not exactly that of a submarine the semi-empirical methods used to calculate the coefficients of the pods will first be verified with captive model test data for the SUBOFF body [8,9] by idealizing the body model. The idealized model body will consist of three simple geometric shapes and is discussed below with the SUBOFF body.

The NCSC method is based on data presented in Reference [10] and gives results consistent with the DATCOM calculations [6] for the SUBOFF body [8, 9]. The DATCOM method is used for slice pod calculations because of ease of programming for parametric studies without requiring coefficients and correction factors derived from graphical techniques. Results of the calculations presented in [6] for methods not used

but considered will be presented for the SUBOFF [8] body without outlining the calculation procedures or details.

C. SUBOFF MODEL

David Taylor Research Center (DTRC) has designed the Defense Advanced Research Projects Agency (DARPA) SUBOFF model 5470 and 5471 described in Reference [9]. The hydrodynamic coefficients, as determined by captive-model tests are shown in [8] and will be used for comparison purposes. In this comparison the reference point (x_m) is located at the body's center of gravity as opposed to it's amidships length as used for the slice pods. The planform of the DARPA model 5470 is shown in Figure 6 [10].

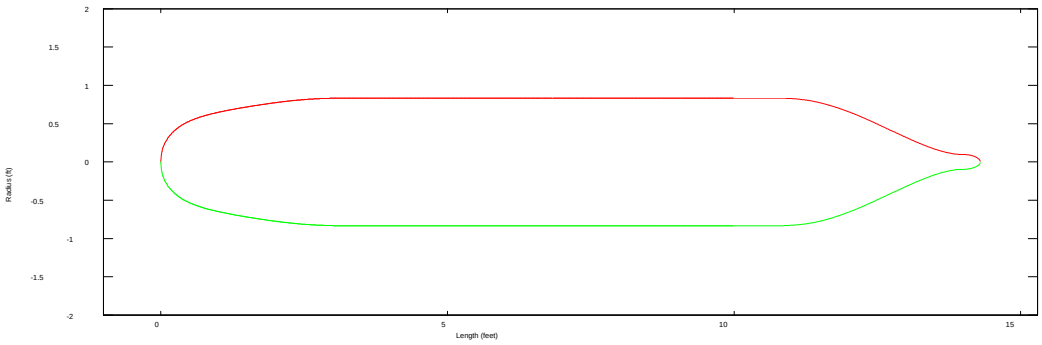

Figure 6. SUBOFF Body [9]

NCSC [10] uses a simplified body of revolution for estimation of the hydrodynamic coefficients which very closely resembles the SLICE pod planform. It

consists of an elliptical nose, a cylindrical or parallel mid body section and a conical base section [10]. Figure 7 shows the simplified body used for estimation of the hydrodynamic coefficients.

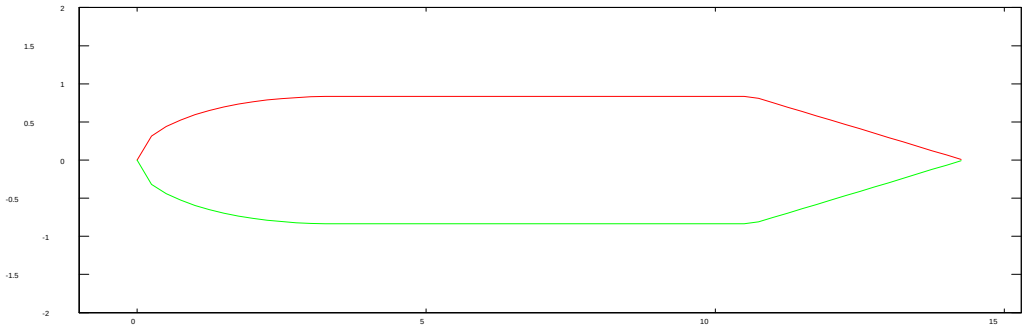

Figure 7. Approximate SUBOFF body. [10]

D. HYDRODYNAMIC COEFFICIENT CALCULATIONS FOR PODS

Y'_v : Calculation of the body alone normal force coefficient using the DATCOM and NCSC methods are similar in nature and form but vary in the method whereby the axial position on the body where the flow becomes predominantly viscous is measured. The Air Force DATCOM method is based on aircraft and missile data and is measured form the nose of the body and is determined from the empirical relation. [6]

$$l_v = 0.378\, l_B + 0.527\, l_{ms} \tag{6}$$

where l_v is the distance from the nose of the vessel to the point where the flow becomes predominantly viscous, l_B is the overall length of the body and l_{ms} is the distance from the nose of the body to the point of maximum slope on the tail section. In the case of a

conical tail the point of maximum slope is at the tip making $l_{ms} = l_B$ in this case and for the SLICE pod. [6]

The lift-curve slope is computed from

$$C_{l\alpha} = 2(k_2 - k_1)\frac{S_v}{S_b} \tag{7}$$

where $C_{l\alpha}$ is the lift slope curve, k_2 and k_1 are the Lamb's coefficients of inertia for a prolate ellipsoid in axial and cross flow respectively. S_v and S_b are the cross sectional areas of the base at point l_v and S_b is the maximum cross sectional area of the body. [6]

The normal force/angle of attack curve slope is calculated as

$$\left(Y'_v\right)_{pod} = \frac{-S_b}{l^2}[C_{l\alpha} + C_{Do}] \tag{8}$$

where C_{Do} is the drag coefficient of an elliptical form at a zero angle of attack and l is the total length of the pod. [6]

N'_v: Body alone yawing moment coefficient calculations presented by Peterson [6] show very good correlation with experimental data for all methods. The NCSC and NSRDC calculations gave the best correlation with the SUBOFF body. However, the data presented in [9] is too limited for SLICE pods and the NSRDC method [6] requires knowledge of the mass of the body. The DATCOM method is used as follows [6].

$$\left(N'_v\right)_{pod} = \frac{C_{m\alpha} S_b}{l^2} \tag{9}$$

where C_{ma} is the yawing moment curve slope and is calculated as

$$C_{m\alpha} = \frac{2(k_2 - k_1)}{S_b l} \int_0^{l_v} \frac{dS}{dx}(x_m - x)dx \tag{10}$$

where S is the cross sectional area of the body as a function of x (S=S(x)) and x_m is the moment reference point for the submerged body [6].

Y'_r, N'_r : Body Alone rotary derivatives calculated with the DATCOM and NCSC methods are identical in form except for the calculation of the point of viscous flow separation as discussed above. The DATCOM method is [6].

$$(Y'_r)_{pod} = C_{l_\alpha}\left(1 - \frac{x_m}{l}\right)\left(\frac{S_b}{l^3}\right) \tag{11}$$

$$(N'_r)_{pod} = \left[\frac{\left(1 - \frac{x_m}{l}\right)^2 - \frac{V}{S_{tb} l}\left(\frac{l_c - x_m}{l}\right)}{\left(1 - \frac{x_m}{l}\right) - \frac{V}{S_{tb} l}}\right] * \left(\frac{-S_b}{l^2}\right) \tag{12}$$

where V is the displacement volume of the submerged body and l_c is the distance from the nose to the center of buoyancy. S_{tb} is the area of the truncated base l_v. [6]

Acceleration hydrodynamic coefficients used for the SLICE pods are based on the works of Humphreys and Watkinson [7] and calculated as follows

$$\left(Y'_{\dot{v}}\right)_{pod} = \frac{k_2 V}{\frac{1}{2} l^3} \tag{13}$$

$$\left(N'_{\dot{r}}\right)_{pod} = -k_b I'_{zdf} + Y'_{\dot{v}}\left(\frac{l_{cb} - l_{cg}}{l^2}\right) \tag{14}$$

where k_b is Lamb's coefficient of added moment of inertia for a prolate ellipsoid body. I_{zdf} is the mass moment of inertia of the displace fluid about the z axis. Terms l_{cb} and l_{cg} are distance from the nose to the center of buoyancy and center of gravity [7]. Table 1 shows the results of the above calculations for the SUBOFF body.

	Experiment	**DATCOM** / % *error*	**NCSC** / % *error*	**NSRDC** / % *error*
Y'_v	-0.005948	-.005836 *-2.473%*	-0.007106 *19.47%*	-.007555 *27.02%*
N'_v	-0.012795	-.013550 *5.90%*	0.012693 *-199.2%*	.012693 *-199.2%*
Y'_r	0.001811	-0.001473 *-181.34%*	-0.002038 *-212.53%*	-0.003259 *-279.96%*
N'_r	-0.001597	-0.001183 *-25.92%*	-0.001628 *1.94%*	-0.001405 *-12.02%*
Y'^*_v	-0.013278	-0.015272 *15.02%*	n/a	n/a
Y'^*_r	.000060	0	0	0
N'^*_v	.000202	0	0	0
N'^*_r	-0.000676	-0.000694 *2.66%*	n/a	n/a

Table 1**.** Comparison of semi-empirical methods of determining hydrodynamic coefficients**.**

E. SLICE POD MODEL

The model used to represent the SLICE pods is closely approximated by a 36 ft long 8 ft diameter body of rotation in the format described above. It consists of an elliptical nose 6 ft long, with a parallel mid-body section 14 ft long with a conical base 16 ft long as shown in Figure 8**.**

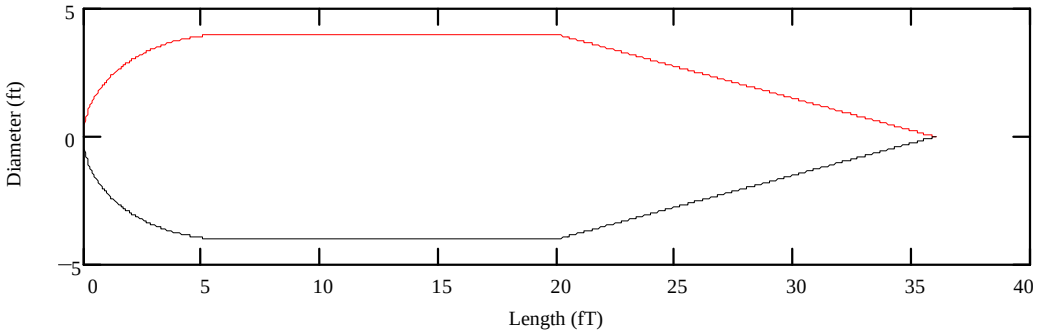

Figure 8. Profile of SLICE pod.

Calculations of the hydrodynamic coefficients of the SLICE pods are done using methods of [6] and [7] for each pod without fins and based on a reference point (x_m) at the mid length of the pod. Reference point x_m for the pods is eighteen feet ($l_B/2$). Pod and strut coefficients, when calculated individually will be non-dimensionalized with respect to pod length (l_B) and later re non-dimensionalized with respect to the vessel length between perpendiculars (L_{bp}).

III. HYDRODYNAMIC COEFFICIENTS OF STRUTS

A. DESCRIPTION

The struts connecting the pods to the body of the SLICE vessel are modeled as flat plates twenty four feet in length, six feet in depth with a zero taper ratio and zero sweep back angle (Λ). Figure 9 shows the baseline strut/pod configuration used in the modeling process.

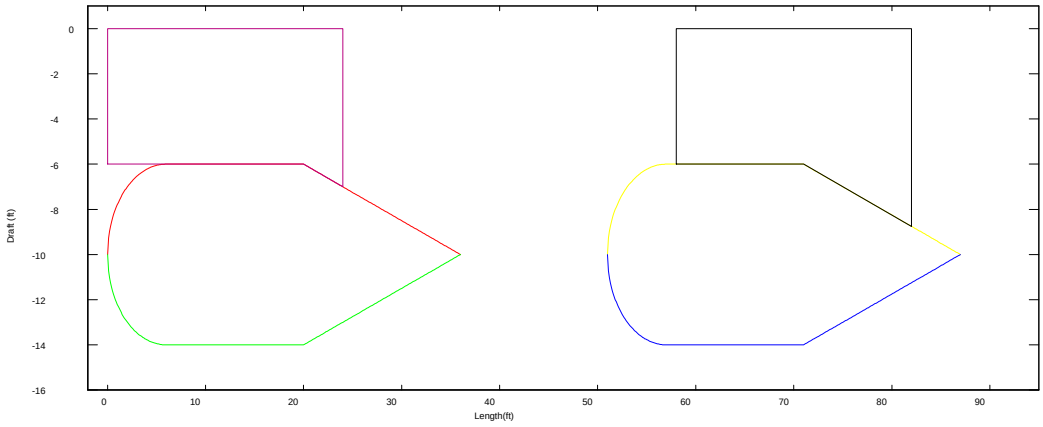

Figure 9. Baseline strut/pod configuration for SLICE model.

The hydrodynamic derivatives for the struts are determined in two parts for each strut. The first part is the fin section formed where the base begins to taper and the second is the six by twenty-four portion which makes up the majority of the strut. Each part is modeled as a flat plate fixed fin located at a distance x_f from the center of the pod to the quarter chord point of the fixed fin. Once the hydrodynamic coefficients are calculated for each strut/pod configuration individually they are translated to the reference point of the vessel and added. At this point in the modeling process the coefficients for the pod and strut are non-dimensionalized with respect to the length of the pod. [3]

B. CALCULATION OF THE HYDRODYNAMIC COEFFICIENT CONTRIBUTIONS FOR A SINGLE STRUT/POD CONFIGURATION

The contributions to the hydrodynamic derivatives of a fixed fin are derived in [3,4] and result in the following

$$Y_{vf} = -A'\left(\frac{\partial C_L}{\partial \alpha} + C_D\right) \tag{15}$$

Where A' is the non-dimensional area of the fin, $dC_L/d\alpha$ is the lift-angle of attack (α) slope curve. C_D is the profile drag coefficient for a flat plate at zero angle of attack and is taken as zero for fins and rudders. Subscript f denotes a fin or rudders. For large ships with relatively small rudders or fins the location of the point of application of the forces is ignored and x_f is taken as the distance from the ship's reference center to the half chord point of the fin [3,4]. Because of the large size of the struts relative to the length of the vessel it is felt that this additional distance cannot be ignored. Theoretically, the point of application of the hydrodynamic force on a flat plate fin with zero taper angle is at the quarter chord point [11].so that when taking the moment contribution of the fixed fin from the center of the pod x_f is the distance from x_m to the quarter chord point . The distance x'_f is the non-dimensional distance from the pod reference point to the quarter chord point i.e. x_f/L. The contributions of the fixed fin to the pod coefficients are given in equations 3 through 5 and are easily derived by summing forces and moments about point x_m.[3]

$$N'_{vf} = Y'_{vf}\, x'_f \tag{16}$$

$$Y'_{rf} = x'_f\, Y'_{vf} \tag{17}$$

$$N'_{rf} = Y'_{vf}\, x'^2_f \tag{18}$$

The acceleration coefficient of a flat plate under lateral acceleration is

$$Y'_{vf} = \frac{-\pi b'^2 l'^2}{\sqrt{\left(a_G^2 + 1\right)}} \tag{19}$$

Coefficients a and a_G in equations 2 and 6 are the effective aspect ratio and effective geometric aspect ratio respectively. For a fixed fin which is in contact with a hull or groundboard such that flow is not allowed around the tip or root chord the effective aspect ratio is twice the aspect ratio for the fin. In the case of the SLICE struts which pass through the water surface and are in contact with the pod the effective aspect ratio is taken as 2a. [3,4]

Following similar logic for the added mass or acceleration derivatives are shown in equations 7 through 9.

$$N'_{vf} = Y'_{vf}\, x'_f \tag{20}$$

$$Y'_{rf} = Y'_{vf}\, x'_f \tag{21}$$

$$N'_{rf} = Y'_{vf}\, x'^2_f \tag{22}$$

The hydrodynamic coefficients contributions of the strut can now be added algebraically to that of the pod as follows. Subscripts p and f designate the coefficient contributions from the pod and fin or strut respectively. [3]

$$Y'_v = Y'_v)_p + Y'_{vf} \tag{23}$$

$$Y'_r = Y'_r)_p + Y'_{rf} \tag{24}$$

$$N'_v = N'_v)_p + N'_{vf} \tag{25}$$

$$N'_r = N'_r)_p + N'_{rf} \tag{26}$$

Similar logic is followed for the added mass coefficients and is repeated for each of the four strut/pod configurations. [3]

IV. COMPLETE HYDRODYNAMIC DERIVATIVES FOR THE SLICE CONFIGURATION

Translating the hydrodynamic coefficient contributions of each of the four strut/pod configurations is performed by taking force and moments about the reference point of the vessel. Principles of Naval Architecture [3] derives the equations with reference to an arbitrary point on a conventional hull and they are adapted here for a single strut/pod as follows.

$$Y'_v = Y'_v \tag{27}$$

$$Y'_r = Y'_v x'_f + Y'_r \tag{28}$$

where x'_f here represents the distance from the amidships reference point to the reference point of the pods with the correct signs (+ for forward pods, - for after pods)

$$N'_v = Y'_v x'_f + N'_v \tag{29}$$

$$N'_r = Y'_r x'_f + Y'_v x'^2_f + N'_v x'_f + N_r \tag{30}$$

The acceleration derivatives are determined with similiar logic and are not shown here.

The final step in determining the overall hydrodynamic derivatives is to non-dimensionalize with respect to the characteristic length of the vessel (l_{bp}) and algebraically sum all of the contributing components together [3]. Assuming that the

forces on each of the fore and aft strut/pods are equal port and starboard we have for the baseline configuration the coefficients as follows.

$$\left(Y_v\right) = 2\left[\left(Y_v\right)_{fwd} + \left(Y_v\right)_{aft}\right] \tag{31}$$

$$\left(N_v\right) = 2\left[\left(N_v\right)_{fore} + \left(N_v\right)_{aft}\right] \tag{32}$$

$$\left(Y_r\right) = 2\left[\left(Y_r\right)_{fwd} + \left(Y_r\right)_{aft}\right] \tag{33}$$

$$\left(N_r\right) = 2\left[\left(N_r\right)_{fwd} + \left(N_r\right)_{aft}\right] \tag{34}$$

Similiar procedure is followed for the added mass derivatives and will not be shown here.

The results of the above calculations are summarized in Table 2. Note that the non dimensionalization of the pod alone and the two strut/pod configurations are with respect to the length of the pod. The base line vessel is non dimensionalized with respect to L_{bp}.

	SLICE Pod Alone	Fwd strut/pod configuration	Aft Strut/pod configuration	Base line vessel w/o rudders.
Y'_v	-0.016244	-0.019149	-0.020316	-0.078930
Y'_r	-0.002498	-0.002518	-0.001135	-0.004044
N'_v	-0.038754	-0.005614	-0.004231	-0.016428
N'_r	-0.006396	-0.000576	-0.000257	-0.010332
$Y'_{\dot{v}}$	-0.044189	-0.012682	-0.012982	-0.051328
$Y'_{\dot{r}}$	0.0	-0.001346	0.005860	0.005617
$N'_{\dot{v}}$	0.0	-0.001305	-0.005860	-0.001945
$N'_{\dot{r}}$	-0.001799	-0.000221	-0.000070	-0.00564

Table 2. Summary of hydrodynamic coefficients for SLICE vessel.

V. RESULTS AND DISCUSSION

After the hydrodynamic coefficients for the base line configuration are calculated the stability eigenvalues of the equations of motion are calculated to be negative real values -0.089 and -1.208. These values indicate that the base line configuration without fins is inherently stable due to the large fin area associated with the struts in agreement with the SWATH results [1]. A parametric study was then conducted to study the effects of moving the struts toward and away from the reference point. The results were as expected, the eigenvalues become more negative indicating increased vessel stability and a related increase in the moment necessary to initiate a turn. [1,3]

Three rudder configurations are studied. The first is a pair of rudders attached to the trailing edge of the after strut without deadwood or attaching structures. The second is a rudder attached to the rear of the after pod without any deadwood and the third is a rudder as a portion of a deadwood attached to the rear of the after pod. At this point no attempt is made to simulate any interference effects from fins, fixtures, hinges or any additional structure necessary to affix the rudder or deadwood to the vessel. Additionally no effort is made to establish the pressure effects between the pods and their effect on the rudders. The size and aspect ratio of the rudders is varied for each configuration studied with the limiting rudder geometry being the span. The maximum span is limited to 6 feet because it is felt that this would be the largest span rudder that could be put in place on the aft strut. The aft strut has a clearance of 8.5 feet between the water surface and the

pod. This model also assumes that the ship does not pitch or roll thereby keeping the entire rudder submerged.

A. STEADY STATE TURNING ABILITY

Once the inherent stability of SLICE is determined, the effects of rudders are introduced. The rudders, modeled as flat plates, are not affixed to any structure at the root and tip allowing flow across the tip and root of the rudder. Each rudder is assumed to have a full effect on the turning ability because of the large separation between aft struts and neglecting pressure effects between them. Calculation of the hydrodynamic coefficients of the rudder and the struts are performed by the same procedure with two notable exceptions. First, the reference point for rudder effect is measured from and calculated with respect to the vessel reference point. This effectively translates the force and moment effects of the rudder directly to the reference point of the ship. The second exception is based on the assumption that the rudder does not broach the surface or come in close contact with any structure at the tip or root chord. This makes the effective aspect ratio simply **a** vice 2**a** as discussed above [3].

Figure 10shows the tactical diameter in ship lengths (D/L) versus percent rudder area for several constant aspect ratio rudders attached to the trailing edge of the aft strut. The percent underwater (u/w) profile area is the percentage of rudder area (A_r) with respect to design length between perpendiculars and draft ($L_{bp}T$) or $A_r/(L_{bp}T)$. The aspect ratios in Figure 10 increase as curves go down. The top curve is for an aspect ratio of 1

and the lower curve is an aspect ratio of 5. The asterisks (*) represent the limiting rudder span of 6 feet and increases for points moving right on the curves. Rudders with a low aspect ratio will tend to be short and fat extending further aft while a higher aspect ratio rudder will tend to be tall and slender as shown in Figure 10.

The results indicate that this model will have tactical diameters between 4 and 7 ship lengths depending on rudder area and aspect ratio. Conventional mono hulls and current SWATH configurations have rudder areas of between 1 and 3 percent of u/w profile area [1]. For rudder areas in this range Figure 10 indicates that aspect ratios between 1 and 3 would be viable alternatives without consideration for rudder stock moments, rudder bending stresses or rudder protrusions aft of the vessel stern.

Figure 11 shows the controls fixed eigenvalues versus percent rudder area for several constant aspect ratio rudders attached to the aft strut. In each case the aspect ratio is increasing as the curves go down. The upper most curve is for an aspect ratio of 1 and the lower most curve for an aspect ratio of 5. Because the eigenvalues increase (become more negative) with increasing rudder size the vessel's straight line stability is increasing at the cost of decreased turning ability.

In the case of a rudder attached to the rear of the aft pod the resulting steady state turning radius and eigenvalue trends are similar to those discussed above. The only difference is in the magnitude of the values. As expected a rudder on the pod, located further from the ships center of gravity will have an increased turning moment and thereby decrease the turning diameter of the ship. Figure 12 shows that the rudder on the

aft pod will generate a smaller turning circle due to the larger rudder moment and Figure 13 shows the controls fixed eigenvalues for the second rudder configuration. Figure 14 and Figure 15 compares the minimum tactical diameters for the limiting cases represented by the asterisks of figures 10 and 12. The results shown in Figure 10 through Figure 13 are reasonably good qualitative descriptions of the stability but do not clearly indicate the interaction between the turning ability and course stability of SLICE.

Biancardi [12] in a study of a data base of 173 vessels of various configurations quantified the dominant eigenvalue for vessels which displayed satisfactory turning ability[12]. It shows that the dominant eigenvalue for both the bare hull and hull and rudder configurations were stable and had good turning ability if the dominant eigenvalue was between -.331 and zero. Dominant eigenvalue less than -.331 indicates stable hulls but with reduced turning ability. Vessels with positive eigenvalues were unstable [3,4,11]. [12]

Figure 16 and Figure 17 show the dominant eigenvalue (σ_2) versus rudder percent area for strut mounted and pod mounted rudders respectively. The asterisk's show the limiting span as described above. Based on [12] the curves indicate that both rudder configurations will result in adequate stability and turning ability for all aspect ratios up to and beyond the limiting span selected.

Case three, a rudder with deadwood attached to the pod is predicted based on the turning characteristics in the previously discussed figures. The deadwood is modeled as a flat plate fixed fin at the aft pod with an eight foot span corresponding to the maximum

diameter of the pod and an aspect ratio of three yielding a deadwood chord of 2.67 feet. Rudder size for this configuration is limited to a span equal to that of the deadwood. Figure 18 is the D/L versus percent rudder area for the third case and clearly show that for a deadwood attached to the aft pod the turning ability is markedly decreased. The dominant eigenvalue for this configuration is -.321 for all aspect ratio's and rudder areas indicating that the vessel is stable but will have poorer turning performance when compared the first two configurations with greater (less negative) eigenvalues.

B. COURSE KEEPING AND TURNING ABILITY, NOMOTO'S FIRST ORDER MODEL

Nomoto presented a simplified analysis of steering system dynamics by manipulating the linearized steering system equations of motion. He developed the first order equation for the yaw rate, given in terms consistent with modern control engineering given in equation 35. [4]

$$\frac{r'}{\delta} = K'\left(1 - e^{\frac{-t}{T'}}\right) \tag{35}$$

where

$$T' = \frac{I'_{zz} - N'_{\dot{r}}}{N'_r} \tag{36}$$

$$K' = \frac{N'_{\delta}}{N'_r} \tag{37}$$

The indices K’ and T’ represent the ratios of non-dimensional coefficients as the yaw inertia /yaw damping coefficient and the turning moment/yaw damping coefficients respectively. [4]

Equation 35 shows that the yaw rate r’ can be represented as a first order system with gain K’ and time constant T’. In steady state the yaw rate per length (r’ = r/L) is simply K’δ. A larger gain, K’ provides a greater steady state turning ability i.e. increased steady state yaw rate, while an increased value of 1/T’ (smaller time constant) will provide a quicker response to the rudder. In addition to indicating the response to the rudder T’ can also provide an indication of the ships course stability. Since a quick response to rudder order is desired in a course keeping / control situation an increased value of T’ is also a quantitative indication of the ship’s course stability. [4]

Figure 19 shows the turning system gain (1/K’) and time constant (1/T’) for constant rudder areas based on the Nomoto first order approximation for a rudder on the aft strut. Each curve represents a constant area rudder with the higher, steeper curves to the left representing small area while the low, shallow curves to the right are higher rudder area. The area limits represented are between five square feet and thirty five square feet in five square foot increments with the maximum span of six feet. Rudder span decreases as the points move upward on the curve with a corresponding increase in rudder chord and decreasing aspect ratio. The data in Figure 19 show that for a given area rudder, a decrease in aspect ratio as we move up the curve will decrease the turning rate (decrease in K’) of SLICE but with a corresponding increase in the sensitivity to

rudder commands and course stability. It is also readily seen that increasing the rudder area will increase both course stability and responsiveness to rudder commands. However in terms of rudder response and course stability the range of 1/T' shown is very small indicating that the course stability is relatively constant for a large range of rudder sizes and corresponds well with the eigenvalue view of stability discussed previously.

Figure 20 is the first order gain and time constant (1/K' -1/T') curve for case 2. The primary difference between the curves in Figure 19 and Figure 20 is found in the value of T for a given rudder area. A rudder attached to the pod will have smaller time constant than a rudder attached to the strut indicating a better response to rudder commands. Additionally this shows that for either rudder configuration of a given area, course stability is not very sensitive to changes in rudder size.

VI. CONCLUSIONS

Based on the linearized model presented herein the SLICE hull has a very good turning ability as well as course stability as shown by the steering system eigenvalues and first order Nomoto model. The results discussed clearly indicate that the turning ability is enhanced with a rudder place further aft or made larger but as in all engineering endeavors, trade offs and practical considerations must be taken in to consideration. Low aspect ratio rudders (aspect ratio 1 or 2) should be considered only with caution as they may extend too far aft, potentially beyond the stern of the ship. They will require more power to operate because of the larger moments about the rudder stock and will have much larger bending stresses associated with them. Very high aspect ratio rudders (aspect ratios four to five or greater) should also be considered carefully as they may often broach the surface of the water in heavy seas, decreasing their effectiveness. The data, based on the model presented supports the use of a strut mounted rudder of aspect ratio between two and four.

As a recommendation for furthur research, we should analyze full scale sea trail data of the SLICE hull and identify the hydrodynamic coefficients. This will enable us to compare the linearized analytical model with experimental results.

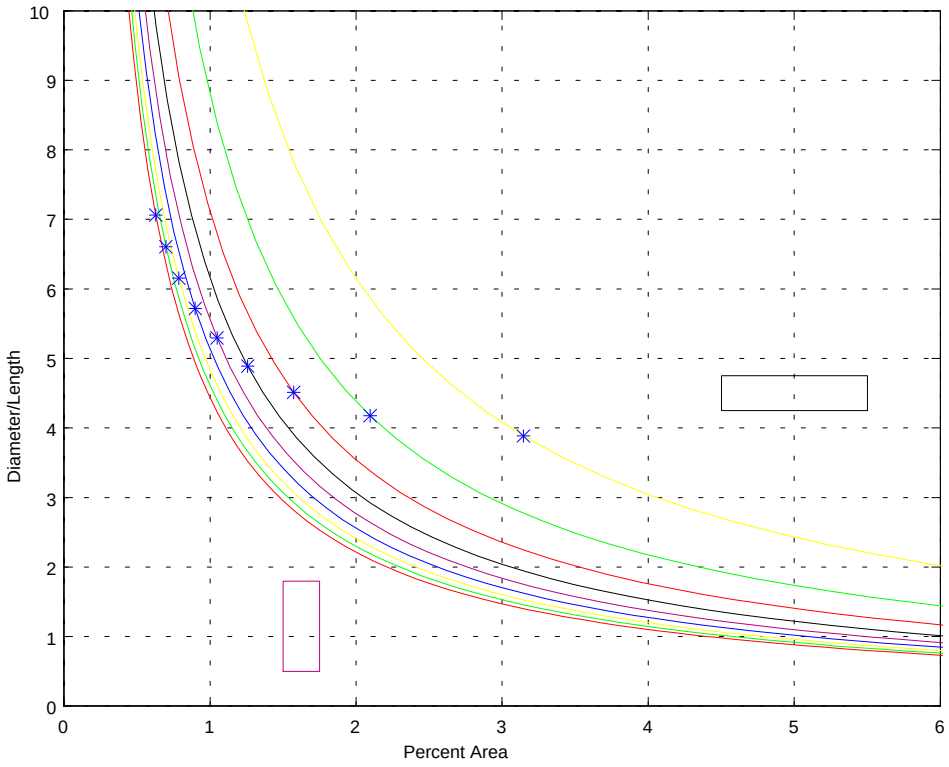

Figure 10. Tactical Diameter (in ship lengths) versus rudder percent area for fixed aspect ratio rudders. Rudders are attached to the trailing edge of the after strut. Asterisks indicate a rudder span of 6 ft.

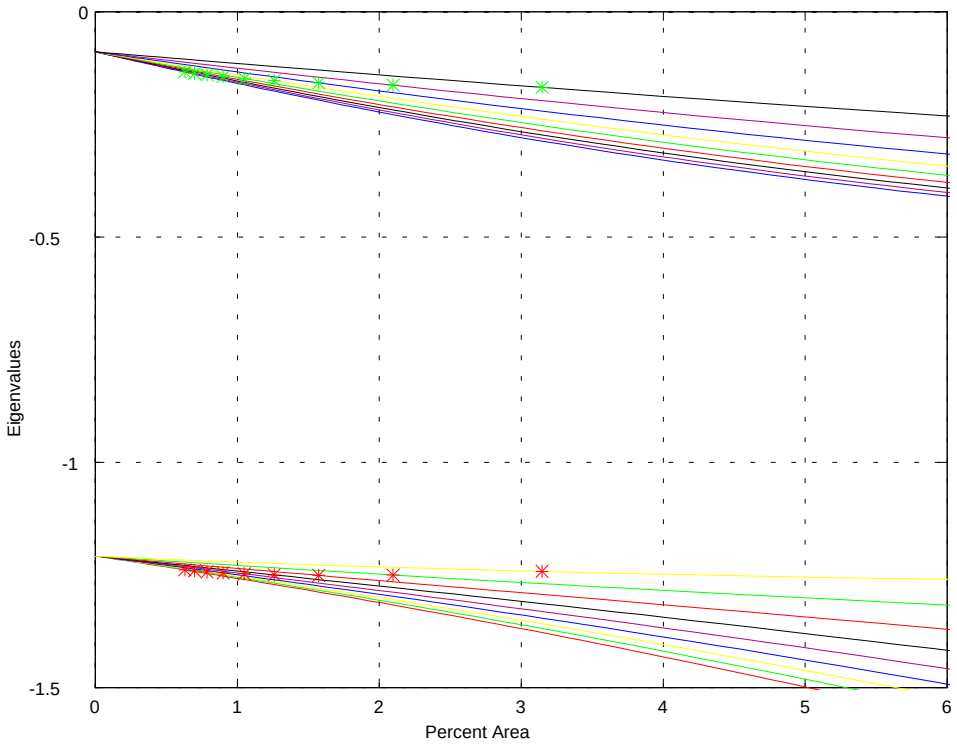

Figure 11. Controls fixed eigenvalues versus rudder percent area for constant aspect ratios. Rudder is fixed to trailing edge of aft strut**.**

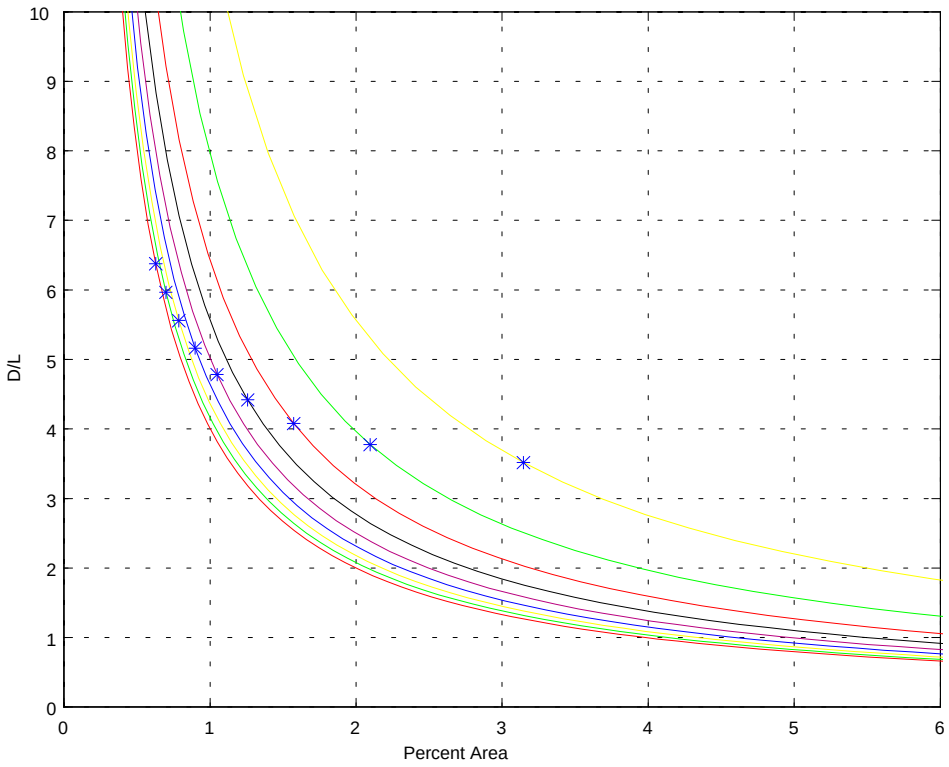

Figure 12. D/L versus rudder percent area for constant aspect ratio rudders. Rudders fixed to back of aft pod.

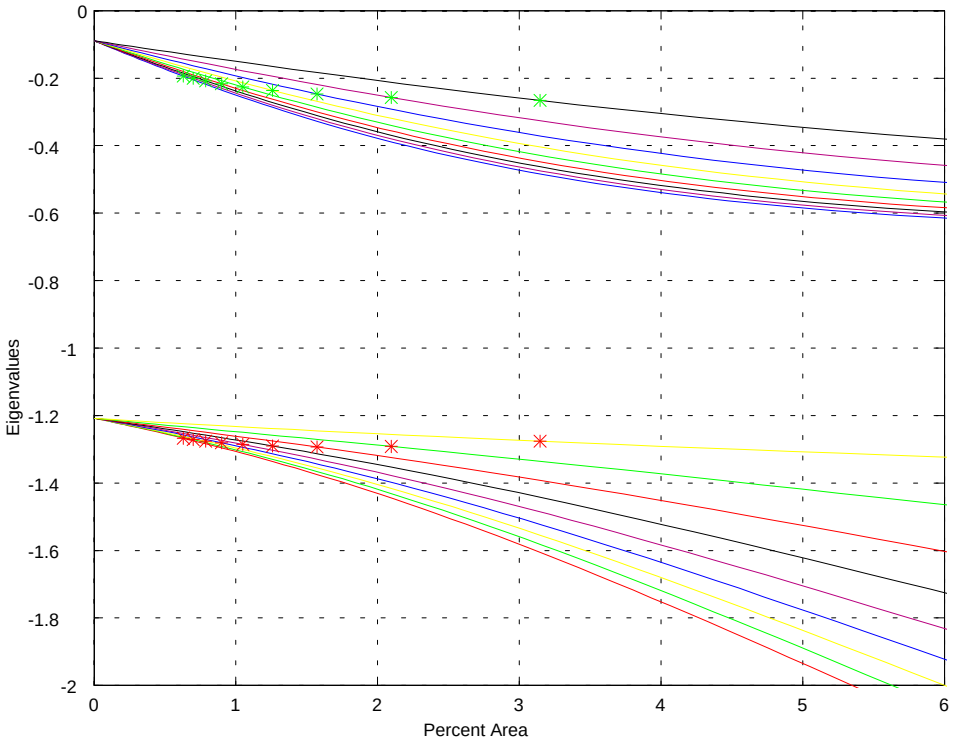

Figure 13. Controls fixed eigenvalues versus rudder percent area for constant aspect ratio rudders. Rudders fixed to rear of aft pod.

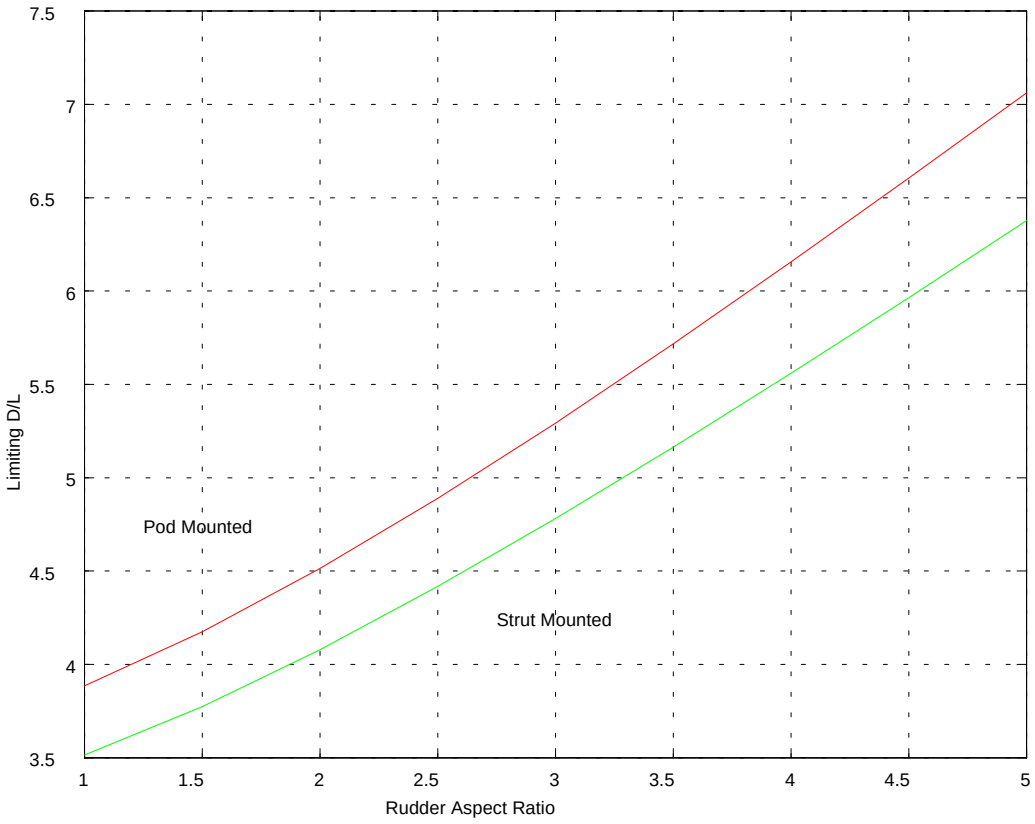

Figure 14. Limiting D/L versus aspect ratio for pod and strut mounted rudders.

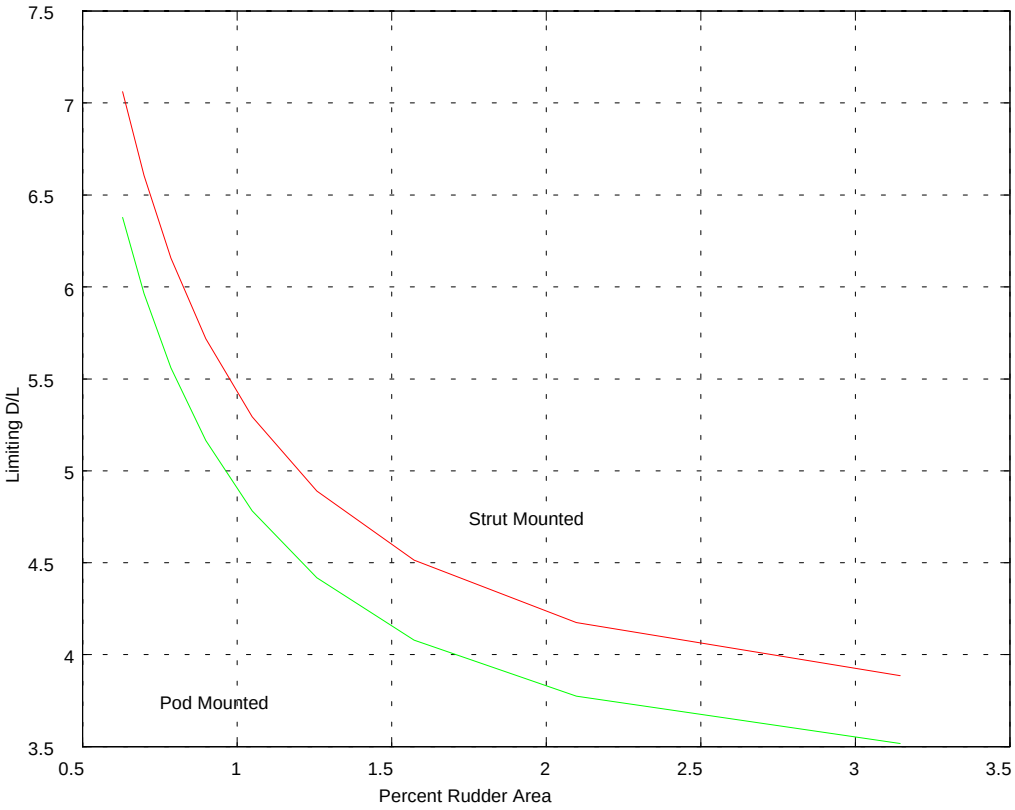

Figure 15. Limiting D/L versus rudder percent area for pod and strut mounted rudders.

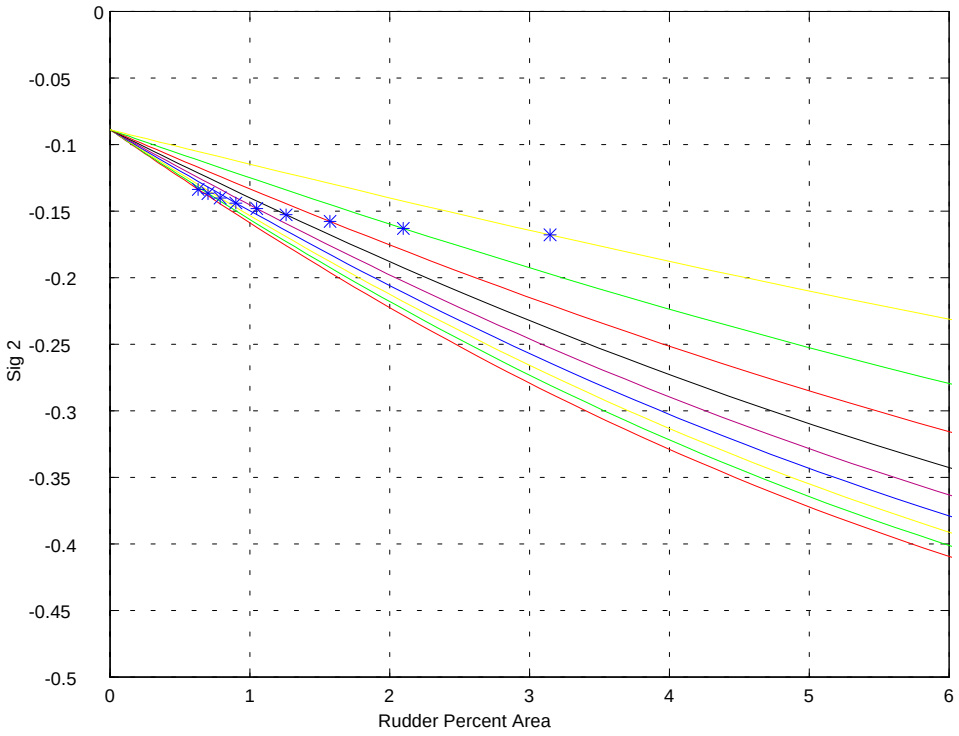

Figure 16. Dominant eigenvalue versus rudder percent area for constant aspect ratio rudders fixed to strut.

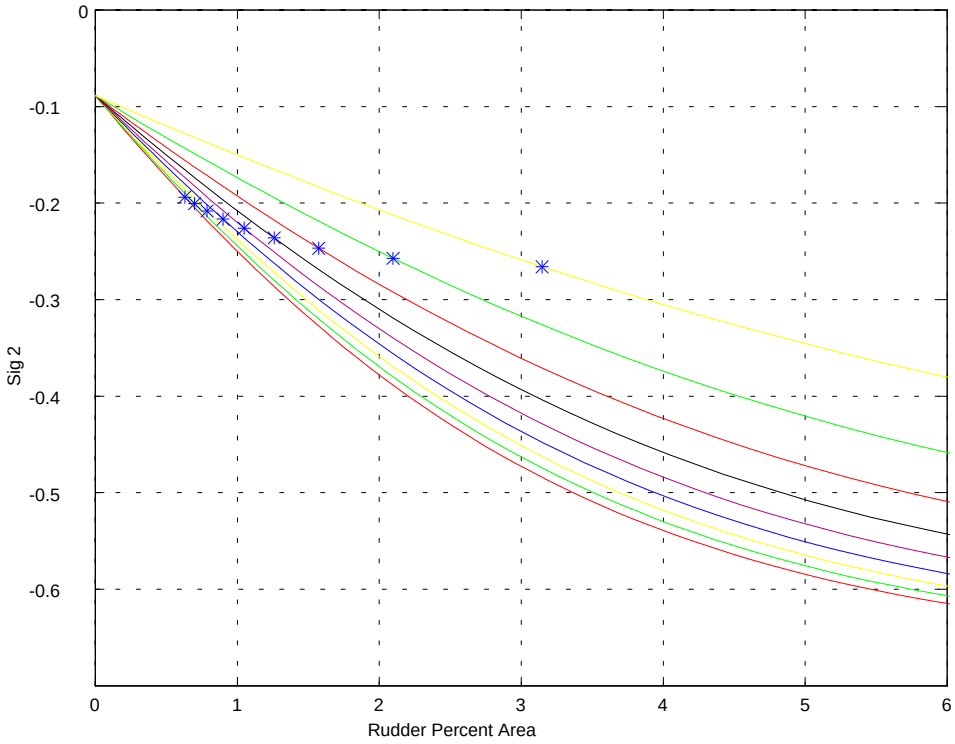

Figure 17. Dominant eigenvalue versus rudder percent area for constant aspect ratio rudders fixed to aft pod.

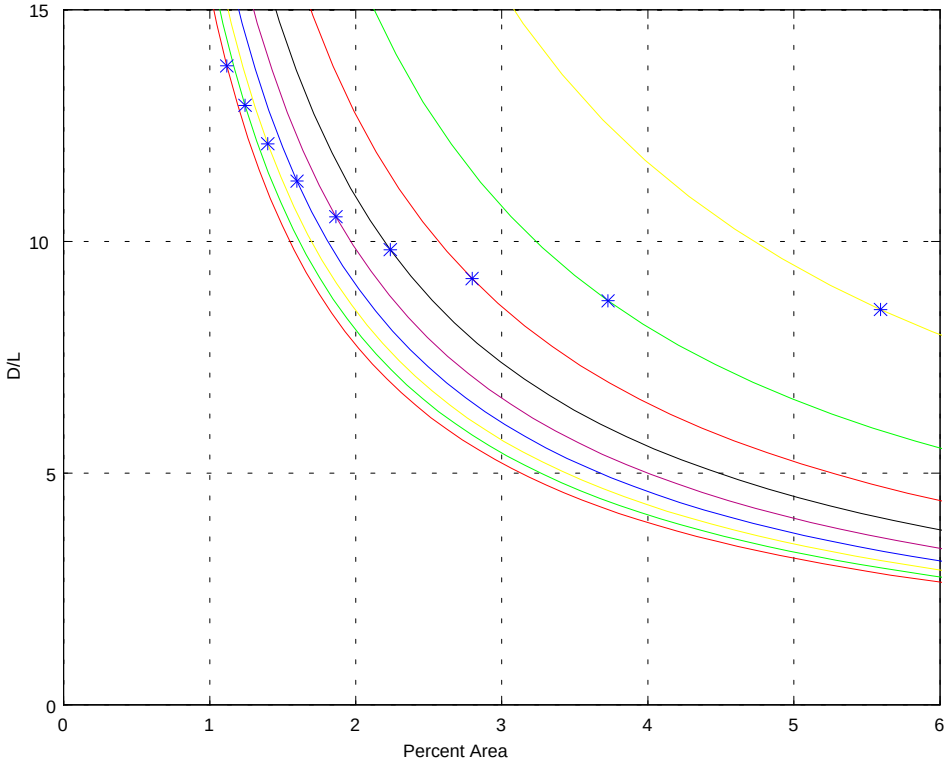

Figure 18. D/L versus percent area for rudder with deadwood attached to pod.

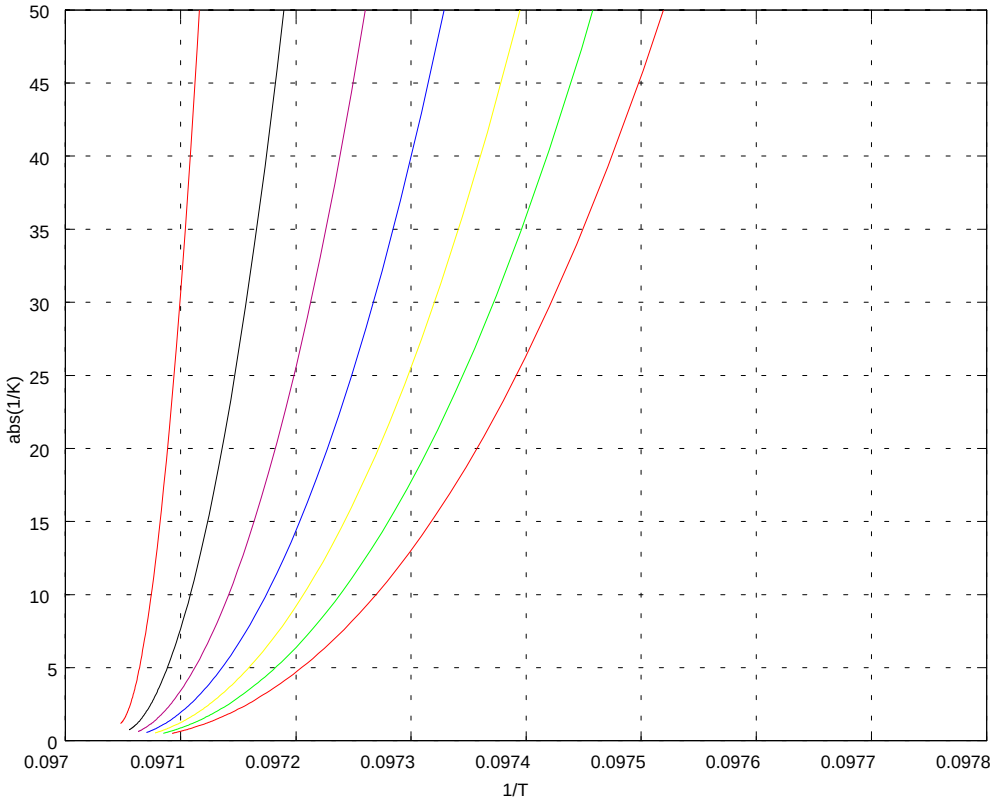

Figure 19. 1/K versus 1/T for constant area rudders attached to trailing edge of aft strut.

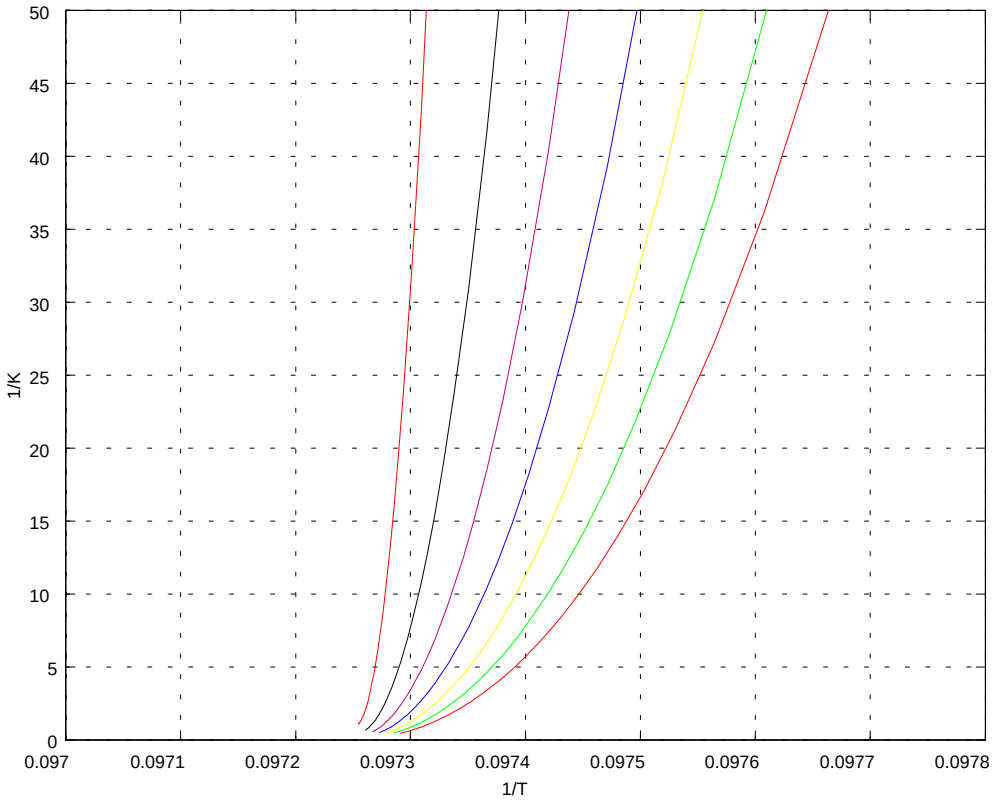

Figure 20. 1/K'-1/T' diagram for constant area rudders fixed to tail of aft pod.

APPENDIX A. SAMPLE CALCULATION OF THE HYDRODYNAMIC COEFFICIENTS OF THE SUBOFF BODY AND SLICE PODS.

APPENDIX B. MATLAB ROUTINE FOR CALCULATION OF THE HYDRODYNAMIC COEFFICIENTS FOR A SINGLE STRUT/POD CONFIGURATION.

```
        function [HCP]=hcsp(L,c,b,xf,fa)
%
%       Hydrodynamic_Coefficients_Slice_Pod
%
%       .m File to calculate the hydrodynamic coefficients of the SLICE
%       pods based on geometric considerations using semi-empirical
%       methods developed by various sources.  (refer to main main
%       document for descriptions of methods.  All coefficients are
%       calculated in dimensionless form using SNAME convention.
%
%       Reference documents are Naval Coastal Systems Center report (NCSC
%       TM-291-80) "Evaluation of Semi-Empirical Methods for Predicting
%       Linear Static and Rotary Hydrodynamic Coefficients" Authored by
%       R. S. Peterson.
%
%       Reference for acceleration Coefficients is
%       Naval Coastal Systems Lab "Prediction of Acceleration
%       Hydrodynamic Coefficients for Underwater Vehicles from Geometric
%       Parameters" (NCSL TR-327-78) by D.E. Hymphreys and K.W. Watkinson
%
% Input Arguments
%
%       L               Column vector of lengths defining body of rotation
%       c,b             Chord and span of flat plate strut.
%       xf,xa   Length(ft) from reference point to 1/4 chord of strut
%       fa              integer flag (1 or 2) to indicate wether fore or aft
%                       strut/pod combination is being calculated
%
% Output Arguments
%
%       HCP     Vector of values as follows
%       HCP(1)          Yv
%       HCP(2)          Yr
%       HCP(3)          Nv
%       HCP(4)          Nr
%       HCP(5)          Yvdot
%       HCP(6)          Yrdot
```

```
%       HCP(7)          Nvdot
%       HCP(8)          Nrdot
%       Coefficients Yrdot and Nvdot are assumed zero for pods
%       because they are generally very small and contribute little.
%
% ********** Start of Executable code **********
%
        load slice
%
% Fill output vector for pod alone non-dimensionalized with respect to
% length of the pod (Calculated in mathcad document "fwdpod.mcd" and
% "aftpod.mcd" which include the effects of the tail as a flat plate.
%
        if (fa == 1)
        %
% Foreward pod coefficients with tail fin as flat plate calculated
% independantly.
%
        Yv=-.017390;            Yr=-.002371;  Nv=-.038626; Nr=-.006268;
        Yvdot=-.044430;         Yrdot=0.000027;
        Nvdot=.000127;                  Nrdot=-.001802;
        elseif (fa == 2)
%
% Aft pod coefficients with tail fin as flat plate
%
        Yv=-.023406;            Yr=-.001105;  Nv=-.037361; Nr=-.005003;
        Yvdot=-.047953;         Yrdot=0.000732;
        Nvdot=.001393;                  Nrdot=-.001941;
        end
%
        HCP(1)=Yv;
        HCP(2)=Yr;
        HCP(3)=Nv;
        HCP(4)=Nr;
        HCP(5)=Yvdot;
        HCP(6)=0;
        HCP(7)=0;
        HCP(8)=Nrdot;
%
% Calculate the coefficients for strut as fixed fin attatched to pod
%
        HCS=hcfps(xf,c,b,T,LB);
%
```

```
% combine and non-dimensionalize the coefficients wrt vessel length
% between perpendiculars.
%
        HCP(1)=HCP(1)*(LB/Lbp)^2        +       HCS(1)*(LB*T)/Lbp^2;
        HCP(2)=HCP(2)*(LB/Lbp)^3        +       HCS(2)*(LB^2*T)/Lbp^3;
        HCP(3)=HCP(3)*(LB/Lbp)^3        +       HCS(2)*(LB^2*T)/Lbp^3;
        HCP(4)=HCP(4)*(LB/Lbp)^4        +       HCS(4)*(LB^3*T)/Lbp^4;
        HCP(5)=HCP(5)*(LB/Lbp)^3        +       HCS(5)*(LB^2*T)/Lbp^3;
        HCP(6)=HCP(6)*(LB/Lbp)^4        +       HCS(6)*(LB^3*T)/Lbp^4;
        HCP(7)=HCP(7)*(LB/Lbp)^4        +       HCS(7)*(LB^3*T)/Lbp^4;
        HCP(8)=HCP(8)*(LB/Lbp)^5        +       HCS(8)*(LB^4*T)/Lbp^5;
```

```
        function [HCS]=hcfps(xf,c,b,T,L)
%
% Hydrodynamic_Coefficients_Flat_Plate_Strut
%
% .m file to calculate the hydrodynamic coefficients of the SLICE
% vessel struts as flat plates placed at a position of xf forward or
% aft of the pod's reference point.  This routine views the struts as
% a fixed fin attatched to the pod with the pressure center acting at
% the point Cmc4 fore (+) or aft (-) of the 1/4 chord point of the fin.
%
% Coefficients are non-dimensionalized as for a surface vessel iaw
% SNAME conventions.
%
% INPUT ARGUMENTS
%
%       xf      Location of center of strut relative to vessel's center
%           reference point.
%       c       Average chord of strut/flat plate (width)
%       b       Span of flat plate/strut
%       T       Draft of vessel (for non-dimensionalization)
%       L       Length of vessel (for Non-dimensionalization)
% OUTPOUT ARGUMENTS
%
%       HCS   Vector of 8 hydrodynamic coefficients in the following order
%       HCS(1)      Yv
%       HCS(2)      Yr
%       HCS(3)      Nv
%       HCS(4)      Nr
%       HCS(5)      Yvdot
%       HCS(6)      Yrdot
%       HCS(7)      Nvdot
%       HCS(8)      Nrdot
%
% LOCAL VARIABLES
%
%       a       Aspect ratio
%       ag      Geometric aspect ratio
%       A       Area
%       Cmc4  Quarter chord moment coefficient
%       Xf      Point of reference for moments
%
% ********** Start of Executable Code **********
%
```

```
% Initialize variables
%
        A=b*c;          % Area of strut
        ag=2*(b/c);             % Aspect Ratio of fin
        a=ag;           %  geometric aspect ratio
        Cla=(0.9*pi*2*a)/(sqrt(a^2+4)+1.8); % Simplified version of eq 23a (pna)
        Cmcl=1/2-((1.11*sqrt(ag^2+4)+2)/(4*ag+2))
        Cmc4=(.25-Cmcl)*(Cla)
        Xf=xf;
        xf,Xf,Cmc4
        Yv=-abs(A*Cla/(L*T));
        Yr=(Xf/L)*Yv;
        Nv=Yr;
        Nr=(Xf/L)^2*Yv;
        Yvdot=-(2*pi*c*b^2)/((L^2*T)*sqrt(ag^2+1));
        Yrdot=-(Xf/L)*Yvdot;
        Nvdot=(Xf/L)*Yvdot;
        Nrdot=(Xf/L)^2*Yvdot;
%
% Fill output vector
%
        HCS(1)=Yv;
        HCS(2)=Yr;
        HCS(3)=Nv;
        HCS(4)=Nr;
        HCS(5)=Yvdot;
        HCS(6)=Yrdot;
        HCS(7)=Nvdot;
        HCS(8)=Nrdot;
```

LIST OF REFERENCES

1. *SWATH SHIPS*, Society of Naval Architects and Marine Engineers, by Colen Kennel, 1992.

2. Lockheed Corporation, *SLICE ADVANCED TECHNOLOGY DEMONSTRATION*, Final Technical Review, 1995

3. *Principles of Naval Architecture,* John P. Comstock editor, Society of Naval Architects and Marine Engineers, 1967.

4.*Principles of Naval Architecture,* v III, Edward V. Lewis editor, Society of Naval Architects and Marine Engineers, 1989.

5. Papoulias, Fotis A. *Informal lecture notes for Marine Vehicle Dynamics ME 4823,* Naval Postgraduate School, Monterey, CA 1993

6. Naval Coastal Systems Center, *Evaluation of Semi-Empirical Methods for Predicting Linear Static and Rotary Hydrodynamic Coefficients,* NCSC TM-291-80, by R. S. Peterson, June, 1980.

7. Naval Coastal Systems Laboratory, *Prediction of Acceleration Hydrodynamic Coefficients for Underwater Vehicles from Geometric Parameters, Naval Coastal Systems Laboratory,* NCSL-TR-327-78, by D.E.Humphreys and K. Watkinson, February, *1978.*

8. David Taylor Research Center, *Investigation of the Stability and Control Characteristics of Several Configurations of the DARPA SUBOFF model (DTRC Model 5470) From Captive Model Tests,* DTRC/SHD-1298-08, by Robert F. Roddy, September, 1990.

9. David Taylor Research Center,*Geometric Characteristics of DARPA SUBOFF Models (DTRC Model Nos 5470 and 5471),* DTRC/SHD-1298-01, by Nancy C. Groves, T. Huang and M.Chang, March, 1989.

10. Naval Coastal Systems Center, *Methods for Predicting Submersible Hydrodynamic Characteristics* , NCSC TM-238-78, by John E. Fidler, and C. Smith, Nielsen Engineering & Research Inc, July, 1978.

11. Biancardi Carmine G. *Principles of a set of Maneuvering Indices Based on Sway / Yaw Phase Relations*. Journal Of Ship Research, Volume 39, Number 2, June 1995.

INITIAL DISTRIBUTION LIST

No. Copies

1. Defense Technical Information Center.....2
   Cameron Station
   Alexandria, Virginia 22304-6145

2. Library, Code 013 2
   Naval Postgraduate School.
   Monterey, California 93943-5002

3. Chairman, Code ME.....1
   Department of Mechanical Engineering
   Naval Postgraduate School
   Monterey, CA 93943-5000

4. Professor Fotis A. Papoulias, Code ME/PA.....6
   Department of Mechanical Engineering
   Naval Postgraduate School
   Monterey, CA 93943-5000

5. Naval Engineering Curricular Office, Code 34.....1
   Naval Postgraduate School
   Monterey, CA 93943-5100

6. LT William J. Wolkerstorfer.....2
   238 Ardennes Circle
   Seaside, CA 93955